JOURNAL OF GEOPHYSICAL RESEARCH, VOL. 113, D00C16, doi:10.1029/2008JD009857, 2008

Modeling of the solar radiative impact of biomass burning aerosols during the Dust and Biomass-burning Experiment (DABEX)

G. Myhre,[1,2] C. R. Hoyle,[2] T. F. Berglen,[2] B. T. Johnson,[3] and J. M. Haywood[3]

Received 25 January 2008; revised 28 August 2008; accepted 9 September 2008; published 27 November 2008.

[1] The radiative forcing associated with biomass burning aerosols has been calculated over West Africa using a chemical transport model. The model simulations focus on the period of January∼February 2006 during the Dust and Biomass-burning Experiment (DABEX). All of the main aerosol components for this region are modeled including mineral dust, biomass burning (BB) aerosols, secondary organic carbon associated with BB emissions, and carbonaceous particles from the use of fossil fuel and biofuel. The optical properties of the BB aerosol are specified using aircraft data from DABEX. The modeled aerosol optical depth (AOD) is within 15–20% of data from the few available Aerosol Robotic Network (AERONET) measurement stations. However, the model predicts very high AOD over central Africa, which disagrees somewhat with satellite retrieved AOD from Moderate Resolution Imaging Spectroradiometer (MODIS) and Multiangle Imaging Spectroradiometer (MISR). This indicates that BB emissions may be too high in central Africa or that very high AOD may be incorrectly screened out of the satellite data. The aerosol single scattering albedo increases with wavelength in our model and in AERONET retrievals, which contrasts with results from a previous biomass burning aerosol campaign. The model gives a strong negative radiative forcing of the BB aerosols at the top of the atmosphere (TOA) in clear-sky conditions over most of the domain, except over the Saharan desert where surface albedos are high. The all-sky TOA radiative forcing is quite inhomogeneous with values varying from -10 to 10 W m^{-2}. The regional mean TOA radiative forcing is close to zero for the all-sky calculation and around -1.5 W m^{-2} for the clear-sky calculation. Sensitivity simulations indicate a positive regional mean TOA radiative forcing of up to 3 W m^{-2}.

Citation: Myhre, G., C. R. Hoyle, T. F. Berglen, B. T. Johnson, and J. M. Haywood (2008), Modeling of the solar radiative impact of biomass burning aerosols during the Dust and Biomass-burning Experiment (DABEX), *J. Geophys. Res.*, *113*, D00C16, doi:10.1029/2008JD009857.

1. Introduction

[2] Uncertainties in the direct radiative effects of aerosols have been reduced considerably over recent years through the combination of aerosol measurement campaigns, and developments in remote sensing and modeling. However, the uncertainty remains substantial [*Forster et al.*, 2007; *Schulz et al.*, 2006]. The northern African continent has a high abundance of aerosols due to emission of dust particles from the Saharan desert and emissions from biomass burning. Previous major aerosol observational campaigns that focus on mineral dust from the Sahara/Sahelian region include the SaHAran Dust Experiment (SHADE), which was based in the Cape Verde Islands off the coast of West Africa [*Haywood et al.*, 2003a; *Myhre et al.*, 2003b; *Tanré et al.*, 2003]. The most significant major international campaign focusing on African biomass burning aerosol was the Southern AFricAn Regional science Initiative (SAFARI 2000) [*Ichoku et al.*, 2003; *Matichuk et al.*, 2007; *Myhre et al.*, 2003a; *Swap et al.*, 2003]. Over West Africa during the dry season, emissions of both biomass burning particles from the Sahelian region and mineral dust particles from the Sahara are significant. The interaction between these two aerosol types and the effects upon the direct radiative forcing is a major focus of investigation during DABEX [*Haywood et al.*, 2008].

[3] Aircraft measurements have shown the biomass burning aerosols to be more absorbing in West Africa during DABEX [*Johnson et al.*, 2008b] than those measured during the Southern African Regional Science Initiative (SAFARI 2000) campaign in South Africa [*Haywood et al.*, 2003b]. In contrast, aircraft measurements of dust during DABEX have shown similar or slightly higher single scattering albedos than those observed in the past during SHADE [*Osborne et al.*, 2008]. Aircraft vertical profiles showed that mineral dust was the dominant aerosol at lower altitudes (0–2 km) and that the biomass burning aerosol was often located above at altitude up to 5 km [*Johnson et*

[1]Center for International Climate and Environmental Research-Oslo, Oslo, Norway.
[2]Department of Geosciences, University of Oslo, Oslo, Norway.
[3]Met Office, Exeter, UK.

0148-0227/08/2008JD009857$09.00

Table 1. Biomass Burning Aerosol Optical Properties From Mie Calculations Based on Aircraft Observations and Those Calculated as Input to the Global Aerosol Model[a]

	ω	k_{ext}	g
Observations (550 nm)	0.81	5.8	0.63
Calculated (550 nm)	0.81	5.8	0.63
Calculated (870 nm)	0.76	2.5	0.46

[a]Aircraft observations are from *Johnson et al.* [2008b]. Aerosol optical properties for single scattering albedo (ω), extinction coefficient (k_{ext}), asymmetry factor, and Ångstrøm exponent (between 550 and 870 nm) are shown. In the observations, ω is based on direct measurements, whereas the k_{ext} and g are calculated using Mie Theory from the observed size distribution.

al., 2008a] owing to the atmospheric dynamics and the position of the ''Harmattan front'' and the intertropical discontinuity (ITD) over West Africa at this time of year [*Haywood et al.*, 2008].

[4] In this study we combine aircraft and ground based measurements with a chemical transport model to calculate the radiative forcing due to biomass burning aerosols during the DABEX campaign. Anthropogenic activity influences the amount of BB aerosols, whereas anthropogenic influence on dust from Sahara is questionable [*Forster et al.*, 2007]. Therefore we restrict in this study to calculate the radiative forcing of BB aerosols.

2. Models

[5] This study uses the global aerosol and chemistry transport model Oslo CTM2, with a spatial resolution of 1×1 degrees and 40 vertical layers [*Berglen et al.*, 2004; *Myhre et al.*, 2007]. This is an off-line transport model using European Centre for Medium-range Weather Forecasts (ECWMF) meteorological data for aerosol transport. For a more thorough model description, see *Berglen et al.* [2004] and *Myhre et al.* [2003a]. The simulations in this study involve a range of aerosol species including mineral dust [*Grini et al.*, 2005], carbonaceous aerosol from fossil fuel and biomass burning [*Berntsen et al.*, 2006; *Myhre et al.*, 2007], and secondary organic aerosols (SOA) [*Hoyle et al.*, 2007]. The model transports the total mass of each of the carbonaceous aerosol species but partitions the dust mass into eight size bins that are transported individually [*Grini et al.*, 2005; *Myhre et al.*, 2003b]. Emissions of primary black carbon (BC) and organic carbon (OC) from biomass burning are predicted from the Global Fire Emission Database version 2 (GFEDv2) [*van der Werf et al.*, 2006]. The BB aerosol is emitted into several model layers within the atmospheric boundary layer to account for the buoyancy of the smoke plumes whereas the other primary aerosols are emitted into the model level closest to the surface only. SOA is formed via the partitioning of semivolatile species to existing organic aerosol. The semivolatile species are formed by the gas-phase oxidation of 12 classes of biogenic and anthropogenic precursors, by either OH, O_3 or NO_3. A two product model [*Hoffmann et al.*, 1997] is used to represent the volatility of the products.

[6] Aerosol optical properties in the Oslo CTM2 are calculated with Mie scattering theory and are used as input for calculations of AOD and radiative forcing. The size distribution and refractive index of the BB aerosol in this study are based on the aircraft measurements of *Johnson et al.* [2008b] from DABEX. The aircraft measurements suggest a size distribution with two lognormal modes and a refractive index of 1.54 + 0.045i. The Mie calculations with these inputs give a single scattering albedo of 0.81 at 550 nm, which matches the aircraft-observed single scattering albedo (SSA) of 0.81 ± 0.05 for aged biomass burning aerosol (Table 1). *Johnson et al.* [2008b] suggest that aged BB aerosols are sufficient for calculating regional radiative forcing because the optical properties of aged and fresh BB aerosols were similar. This assumption is also supported by the study of *Abel et al.* [2003] during SAFARI 2000, who show the single scattering albedo of biomass burning aerosol changes from that typical of fresh aerosol to that typical of aged aerosol over a 5-hour period subsequent to emission.

[7] The extinction coefficient, asymmetry parameter and Ångstrøm exponent used in the model are also in good agreement with those derived from aircraft observations of aged BB aerosols and reported by *Johnson et al.* [2008b] (see Table 1). The optical properties of secondary organic aerosols are assumed to be the same as those of the BB aerosols. The optical properties of mineral dust are also based on Mie theory and size distributions and refractive index are taken from AERONET retrievals. The adopted refractive index is 1.48 + 0.001i at 550 nm, which gives a single scattering albedo close to the observed value of 0.98 ± 0.02 at 550 nm from DABEX [*Osborne et al.*, 2008]. Dust and BB aerosols are treated separately (i.e., as external mixtures).

[8] Radiative forcing calculations are performed with a multistream model using the discrete ordinate method [*Myhre et al.*, 2007; *Stamnes et al.*, 1988]. The model includes treatments for radiative absorption by gases, Rayleigh scattering and scattering by the clouds.

3. Results

3.1. Aerosol Optical Depth

[9] Figure 1 shows the aerosol optical depth (AOD) at 550 nm for the period 13 January to 3 February 2006, for the model and for satellite retrieved AOD from MODIS (Collection 5) [*Levy et al.*, 2007; *Remer et al.*, 2005] on both Terra and Aqua. The retrieved AOD from MISR (version F06_0021) [*Kahn et al.*, 2005] is also shown in Figure 1d, which is the mean of values from January 2006. The model has higher AOD values than MODIS over almost the whole of the studied region. The regional mean AOD at 550 nm over the area 0°N to 15°N and 20°W to 20°E is 0.45, 0.30, 0.30, and 0.33 for the model, MODIS on Terra, MODIS on Aqua, and MISR, respectively. The overestimation compared to MODIS is particularly large in central Africa. MISR shows slightly higher AOD than MODIS and has some indications of very high values in central Africa. Some, but certainly not all, of this difference between the model and the satellite retrievals is likely to be due to the fact that the satellite retrieved AOD from MODIS in the biomass burning region was significantly lower for January/February 2006 than for any other year in the period 2001–2006 [*Derimian et al.*, 2008]. However, there are still discrepancies that need to be accounted for. The large overestimation of AOD in the model over central Africa,

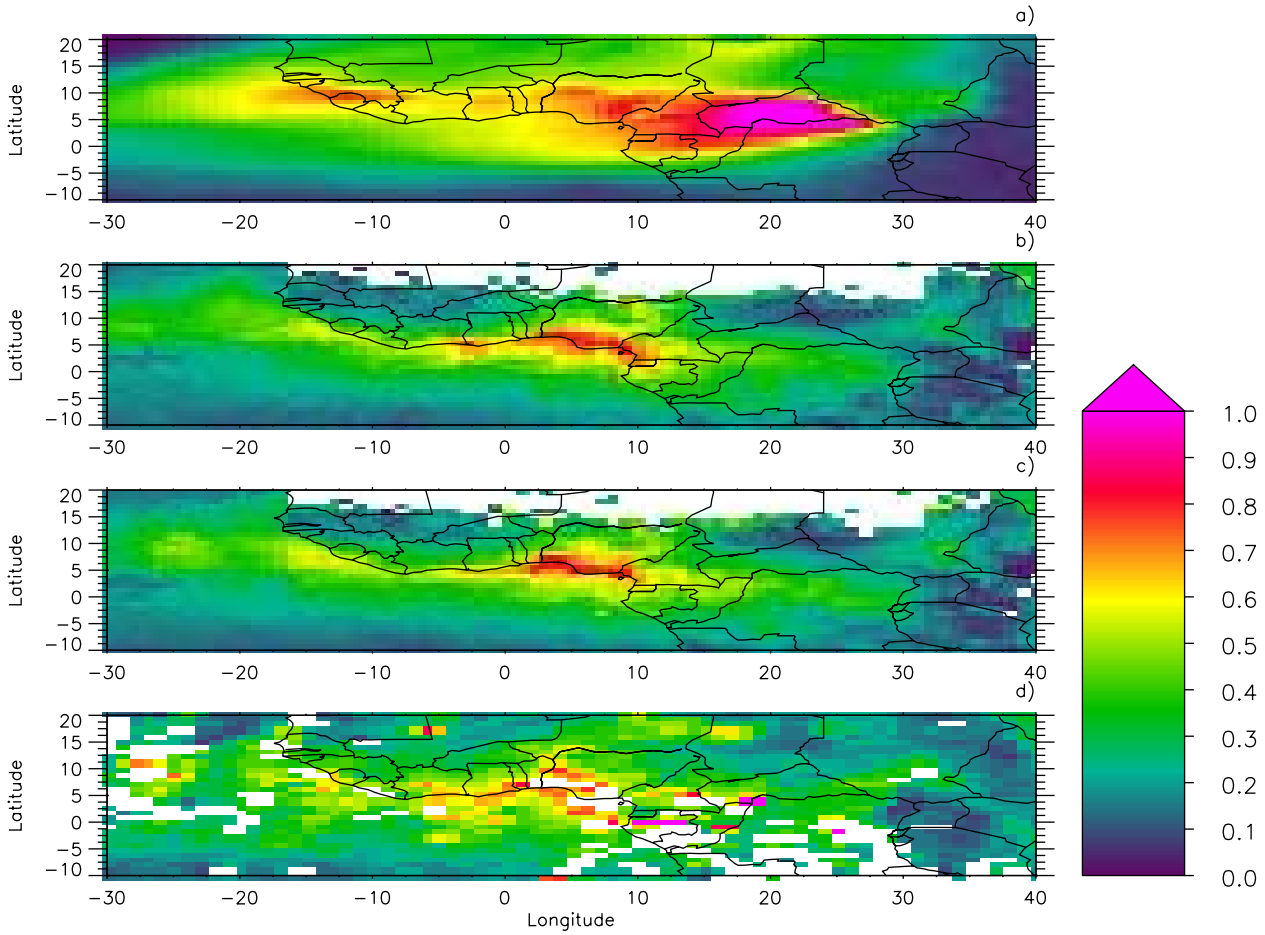

Figure 1. Aerosol optical depth (at 550 nm) from (a) model, (b) MODIS on Terra, (c) MODIS on Aqua, and (d) MISR. The results are shown for the DABEX campaign period from 13 January to 3 February 2006, except for MISR where a monthly mean from January 2006 is shown.

as compared to the satellite data, may be associated with the excessive biomass burning emissions over central Africa in the GFED database. Figure 2 shows very high global fire counts [*Giglio et al.*, 2003] and biomass burning emissions [*van der Werf et al.*, 2006] in a band between 5°N and 15°N over almost the entire Africa. This region has the highest global fire counts and biomass burning emissions worldwide for January 2006 (not shown). The fire counts in Figure 2 have a more evenly distributed pattern than the biomass burning emissions, which are much higher in the equatorial Africa than in the Sahel. This difference is caused by the higher fuel loads in central Africa, as estimated by *van der Werf et al.* [2006]. It is possible that very high AOD values over central Africa are incorrectly identified as cloud and consequently rejected from standard algorithms. Although we discuss MODIS and MISR retrieval products, such a problem has previously been identified for Clouds and the Earth's Radiant Energy System (CERES) Earth Radiation Budget Experiment (ERBE)-like retrievals during a large dust storm (aerosol optical depths of approximately 1.5) off the coast of West Africa during the SHADE campaign [*Haywood et al.*, 2003a]. The infrequent detection of aerosol optical depths greater than one observed by MISR over this region may tentatively support this hypothesis, but further investigation would be necessary for definitive conclusions to be drawn. Another possible explanation is that aerosol optical properties in central Africa may differ significantly from those measured by an aircraft limited to a region near Niamey, Niger during DABEX, whereas our model assumes BB aerosol properties to be the same everywhere in the domain.

[10] Figure 3 compares model AODs against AERONET monthly mean AODs (Level 2.0 and version 2) [*Holben et al.*, 1998] for January 2006 and for five sites in the studied region. For three of the sites the model overestimates the AOD and for the other two sites an underestimation occurs. The model AOD is 45% higher than AERONET at Dakar and 15–20% higher than AERONET at IER Cinzana and Banizoumbou, which are closer to the main BB emission regions. At Ilorin the model underestimates AOD by around 25%. However, the temporal coverage is extremely limited at Ilorin (only 2 days of measurements). At Djougou the model underestimates AOD by less than 10%. The ratio between AODs at 550 and 870 nm are quite similar in the model and the AERONET measurements, which indicates that the relative contributions of BB and mineral dust aerosol are reasonable in the model. This can be inferred because BB aerosols and dust have quite different variations in the AOD with wavelength, as expressed by their different Ångstrøm exponents [*Tanré et al.*, 2003].

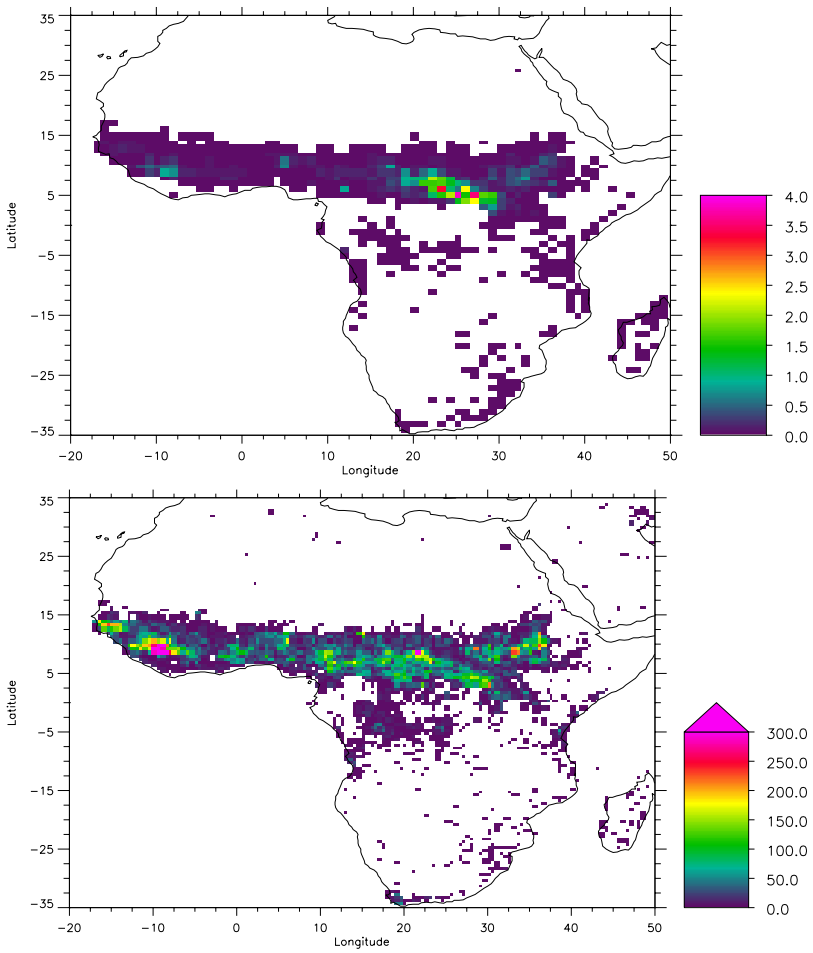

Figure 2. (top) GFED OC emissions (g C/m^2/month) for January 2006 and (bottom) MODIS fire counts for January 2006.

[11] Figure 3 also includes a comparison of model AODs with the satellite data (MODIS and MISR) retrieved over the AERONET sites. The disagreement between model and satellite AOD is much larger than the disagreement between the model and AERONET measurements. The modeled AOD is 40–100% higher than the MODIS data at the five AERONET sites. However, the MODIS AODs are much lower than AERONET at these five sites. The MISR AODs are closer to both the model and the AERONET data, although they are still generally lower than the AERONET data. This analysis shows that the apparent strong overestimation of model AOD inferred from Figure 1 may be partly explained by the MODIS AOD being too low. However, the comparison of monthly mean satellite data with AERONET data as well as with model data is complicated owing to the screening and sometimes limited coverage of remotely sensed data [*Matichuk et al.*, 2007; *Myhre et al.*, 2005].

[12] Figure 4 shows the separate contributions to AOD from the three main aerosol components included in our model simulations (BB aerosol, mineral dust, and carbonaceous aerosols from fossil fuel and biofuel). BB aerosols dominate the AOD around the equator, especially between 5°S and 5°N. Northward of this, mineral dust gradually becomes the dominant aerosol, owing to increasing dust and decreasing BB aerosol. In the region close to Niamey (13.5°N, 2.2°E), where the aircraft was based during DABEX, BB aerosol and mineral dust are both important contributors to the AOD. In contrast, the AOD of carbonaceous aerosol from fossil fuel or biofuel use is rather low in the DABEX region.

3.2. Single Scattering Albedo

[13] The SSA is of crucial importance for the magnitude, and even the sign of the radiative forcing of atmospheric aerosols [*Hansen et al.*, 1997; *Haywood and Shine*, 1995]. The modeled SSA for the DABEX campaign period is shown in Figure 5. The values range from nearly 0.80 in the regions with largest BB emissions, to nearly unity further north where mineral dust is the dominant aerosol type.

[14] Compared to AERONET measurements, the model overestimates SSA by an average of 0.045 for the five stations considered (Table 2). It is unclear whether this overestimation is due to too weak absorption by the BB aerosols or too large a fraction of mineral dust particles. The aircraft measurements were also significantly higher than those from AERONET with column-averaged values around 0.90 at 550 nm near Banizoumbou. Aircraft observations also suggest that mineral dust dominated the aerosol

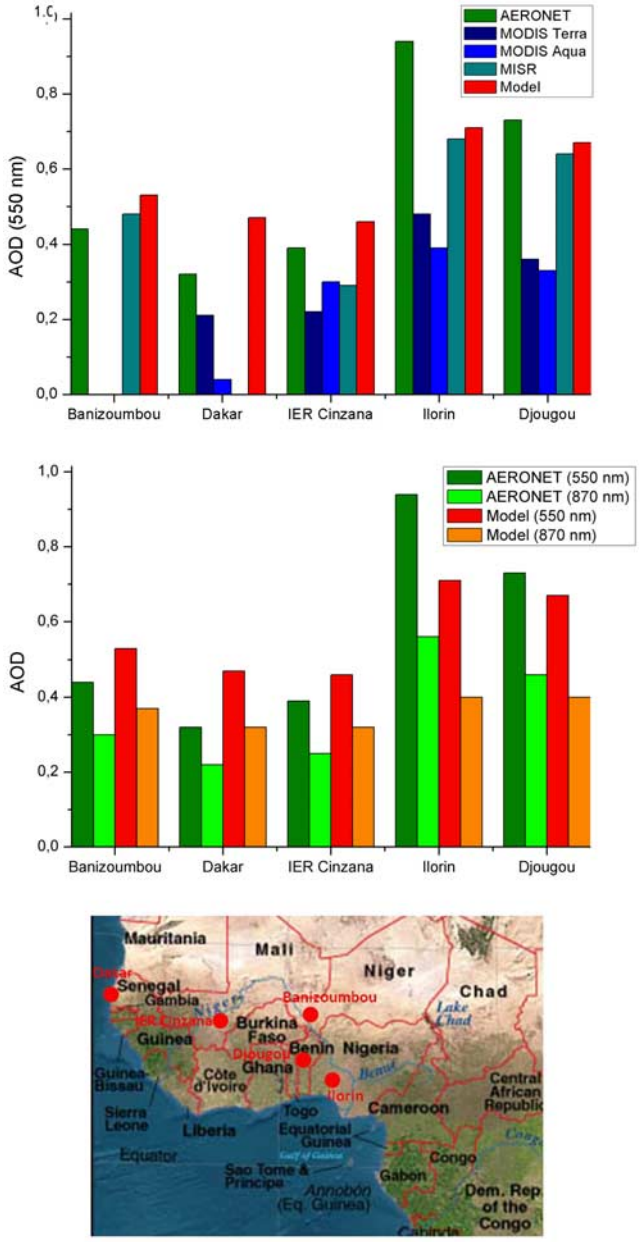

Figure 3. (top) Monthly AOD at 550 nm for January 2006 AERONET, satellite data, and the model and (middle) and AOD at wavelengths 550 nm and 870 nm for AERONET and the model. AERONET data at 550 nm are derived as mean of data at 440 and 670 nm. The number of days with observations is 25, 12, 18, 2, and 20, respectively, for Banizoumbou, Dakar, IER Cinzana, Ilorin, and Djougou. (bottom) Map over western Africa marked with the AERONET stations used in this study. A map with all the measurements sites during DABEX can be found in the DABEX overview paper [*Haywood et al.*, 2008].

column near Banizoumbou during DABEX and that the dust had very high SSA of 0.98–0.99 at 550 nm [*Osborne et al.*, 2008]. The aircraft profiles averaged over the whole campaign showed that dust accounted for about 65% of the optical depth in the Niamey/Banizoumbou region, with the remaining 35% being from BB aerosol [*Johnson et al.*, 2008a]. Therefore the column-average SSA should be closer to that of the dust (0.98) than the BB aerosol (0.81). The discrepancy between the aircraft observations of single scattering albedo and the AERONET observations is, as yet, unresolved [*Osborne et al.*, 2008]. However, it should be noted that in regions of significant dust loading, the derived single scattering albedos are very sensitive to the implicit assumptions in the retrievals. *Osborne et al.* [2008] show that, on swapping from version 1 (an outdated AERONET retrieval algorithm) retrievals of SSA to version 2, over the Banizoumbou site for the cases considered, the single scattering albedo decreases from a mean of 0.94, to a mean of 0.87, indicating an increase of a factor of 2 in the aerosol absorption. Other observations of SSA also indicate higher values than in the measurements from AERONET [*Mallet et al.*, 2008].

[15] The AERONET measurements during DABEX (Table 2) show an increase of SSA with wavelength. This differs from measurements during SAFARI 2000 that showed a clear reduction of SSA with wavelength [*Bergstrom et al.*, 2003; *Eck et al.*, 2003; *Haywood et al.*, 2003b]. Our model also shows increases in SSA with wavelength (Table 2) despite the fact that BB aerosols have a reduction in the SSA with wavelength (see Table 1). This result can be explained by the strong wavelength dependence of AOD for the BB aerosols. The contribution to AOD from BB aerosols decreases rapidly with wavelength so that the BB AOD at 870 nm is less than half the BB AOD at 550 nm (see Table 1). Thus the scattering from the dust particles dominates more strongly for 870 nm since the dust AOD varies very little with wavelength but has a much higher SSA than the BB aerosol. The fact that the model reproduces a rather similar wavelength dependence of the SSA as compared to the AERONET measurements indicates that the relative contributions of mineral dust and BB aerosol are reasonable in the model.

3.3. Aerosol Vertical Profile

[16] Global aerosol models differ significantly in their vertical profiles of aerosols [*Schwarz et al.*, 2006; *Textor et al.*, 2006]. This difference is likely to be important in explaining discrepancies between estimates of direct radiative forcing by aerosols. The global aerosol model Oslo CTM2 compared well in previous comparisons of the aerosol vertical profiles against aircraft measurements for both biomass burning aerosol and mineral dust aerosol [*Myhre et al.*, 2003a; *Myhre et al.*, 2003b]. Figure 6 shows observed and modeled aerosol vertical profiles near Niamey from the DABEX campaign. The observed profile is derived from a TSI nephelometer data from an average from 23 Facility for Airborne Atmospheric Research (FAAM) BAe146 aircraft profiles taken less than 100km away from Niamey. The Ångstrøm exponent is used to partition the aircraft vertical profile between biomass burning and mineral dust [*Johnson et al.*, 2008b; *Milton et al.*, 2008]. The observations show that BB aerosols dominate in the upper part of the aerosol layer and have a rather constant extinction from 1.5 to 5 km (Figure 6, bottom). The dust was observed to have a strong maximum near 1 km and to gradually decrease from 1 to 5km. The model results are shown in Figure 6 (top), and Figure 6 (bottom) shows both the model and observed results. The model results show the

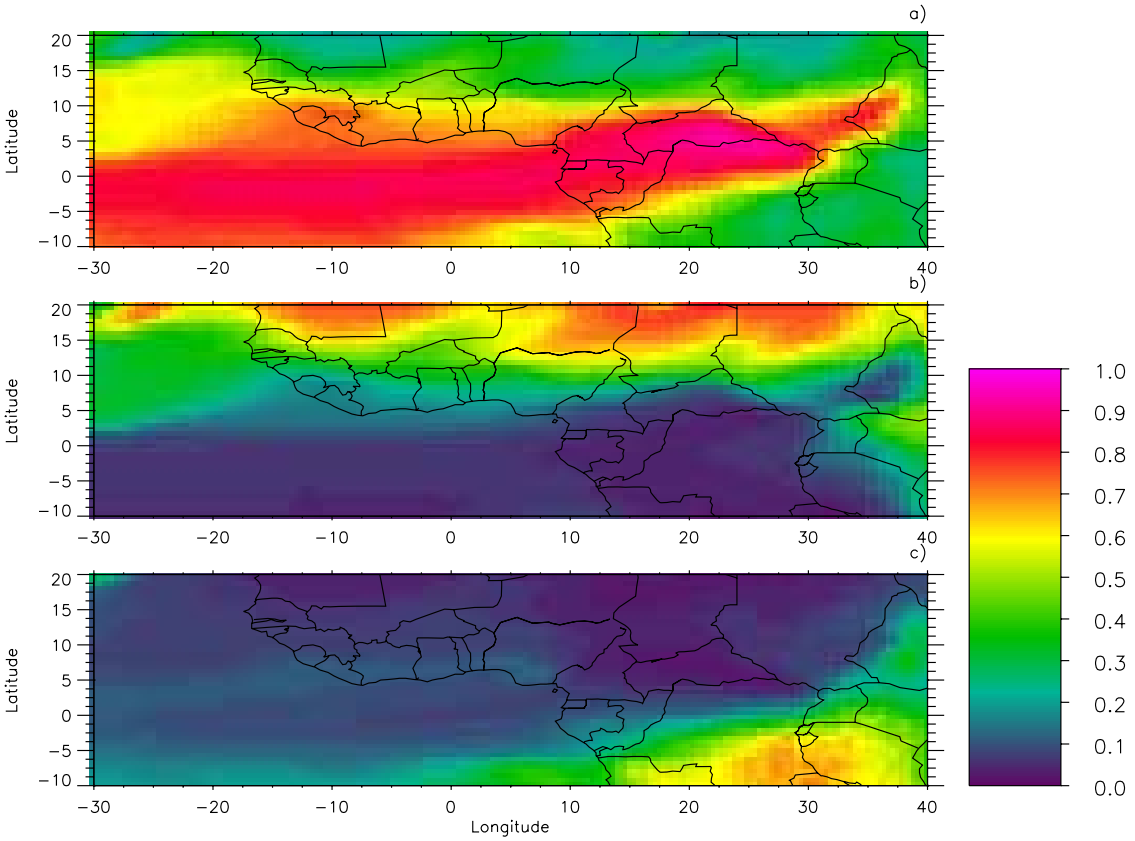

Figure 4. Relative contribution of AOD from Oslo CTM2 during the DABEX campaign from (a) BB aerosols, (b) mineral dust, and (c) carbonaceous aerosols from fossil fuel and biofuel combustion.

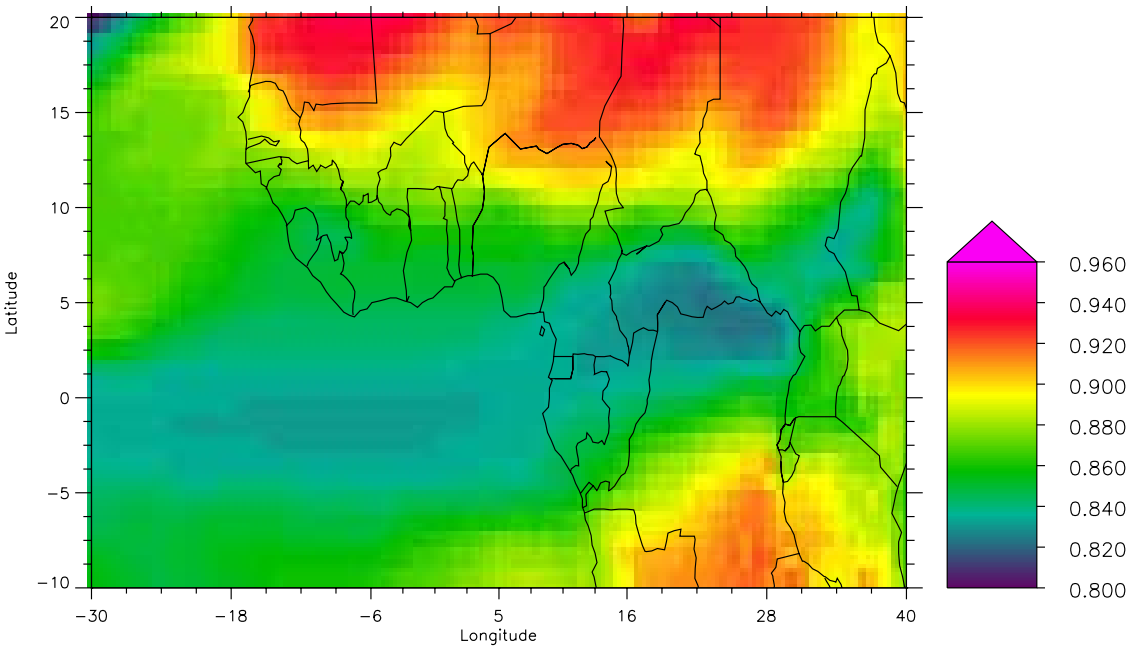

Figure 5. Modeled single scattering albedo during the DABEX campaign period from the mixture of all modeled aerosols (primary BB aerosols, mineral dust, carbonaceous aerosols from fossil fuel and biofuel combustion, plus secondary organics).

Table 2. Monthly Mean Single Scattering Albedos for January 2006 From AERONET Measurements and From the Global Aerosol Model for Monthly Mean Values[a]

	Aeronet		Model	
	SSA 550[b]	SSA 870	SSA 550	SSA 870
Banizoumbou	0.84	0.85	0.89	0.91
Dakar	0.85	0.87	0.89	0.91
IER_Cinzana	0.82	0.84	0.89	0.92
Ilorin	0.84	0.86	0.85	0.85
Djougou	0.82	0.85	0.86	0.87

[a]The number of days with AERONET measurements is the same as for AOD in Figure 3. The location of the AERONET sites can be found on the map in Figure 3.
[b]Data at 550 nm are derived as mean of data at 440 and 670 nm.

upper part of the aerosol layer to consist predominantly of BB aerosols, while dust is more abundant in the lower part. This pattern is consistent with the observations. In the model, part of the carbonaceous aerosols is from fossil and biofuel whereas the observations assume all fine combustion-related particles to be BB aerosol. However, the extinction from non-BB carbonaceous aerosol is quite small. The altitude dependence of the total extinction from all carbonaceous aerosols is of quite similar shape to that in the observations, except that the model simulates aerosols around 1 km higher. There is also a variation in the measured vertical profile below 1 km that is not fully captured by the model. The modeled dust extinction is similar to the observed extinction between 2 and 5 km. However, there are significant discrepancies between model and observation in the lowest 2 km of the profile. The model does not adequately capture the sharp increase in dust extinction in the lowest 2 km or the rapid drop in BB extinction to almost zero at around 1 km.

3.4. Radiative Forcing

[17] Figure 7 shows the radiative forcing at the top of the atmosphere (TOA) from the BB aerosols during DABEX for both clear-sky and all-sky conditions. The radiative forcing is the difference between two radiative transfer simulations including and excluding the BB aerosols (but with mineral dust and carbonaceous aerosols from fossil fuel always included). Under clear-sky conditions the BB aerosols have a strong negative forcing over the ocean, indicating a cooling effect. Negative radiative forcing also occurs over land regions with low surface albedo, for clear-sky conditions. However, the clear-sky radiative forcing changes sign to become positive over the Saharan desert where the surface reflectance is high. Over the Niamey region where most of the aircraft observations were made [*Haywood et al.*, 2008] the radiative forcing is slightly negative, which agrees with the observation-based calculations of *Johnson et al.* [2008a]. When clouds are included in the simulations (Figure 7b), the radiative forcing is substantially less negative; it even changes sign to become positive in several places. This change occurs because the absorption of absorbing aerosols is enhanced above brightly reflecting clouds. This interaction was demonstrated during SAFARI 2000 where elevated layers of BB aerosol gave a positive radiative forcing when there was a high coverage of marine stratocumulus below [*Keil and Haywood*, 2003; *Myhre et al.*, 2003a]. Over the southern coast of western Africa cloud cover is close to 100%, giving a high, positive radiative forcing. Over the arid regions of the Sahara the radiative forcing changes little between clear-sky and all-sky conditions owing to the low cloud fraction there. The change in sign from negative to positive radiative forcing occurs at around 15°N for both clear-sky and all-sky conditions.

[18] The regional mean all-sky BB aerosol radiative forcing, averaged over the domain shown in Figure 7, is slightly positive (+0.06 W m^{-2}), whereas under clear-sky conditions it is −2.4 W m^{-2}. These are viewed as anthropogenic forcings since the vast majority of biomass burning fires in this region are ignited by humans for agricultural purposes. Two sets of sensitivity simulations have also been performed. In the first sensitivity test the single scattering albedo is reduced by 0.08 from 0.81 to 0.73 at 550 nm (the minimum value observed during DABEX [*Johnson et al.*, 2008b]). In the second sensitivity test the concentration of mineral dust below 2 km was increased by a factor of 4, following the comparisons in Figure 6. In the simulation with reduced single scattering albedo the regional mean

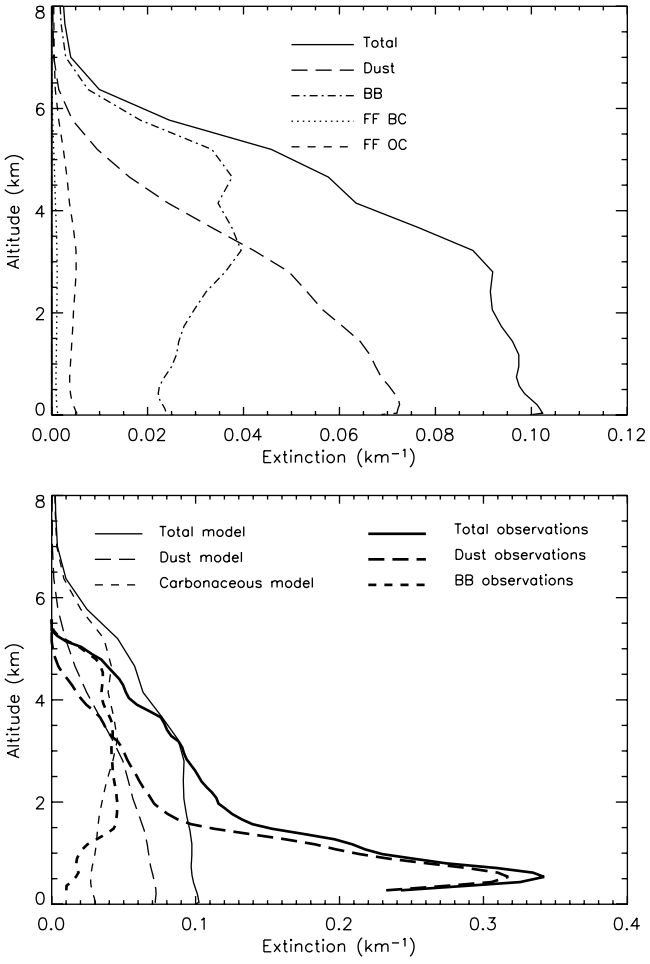

Figure 6. Vertical aerosol profile from (top) the aerosol model and (bottom) both model and observations. The model results for carbonaceous aerosols in the bottom panel are the sum of BB aerosols, fossil fuel (FF), black carbon (BC), and FF organic carbon (OC).

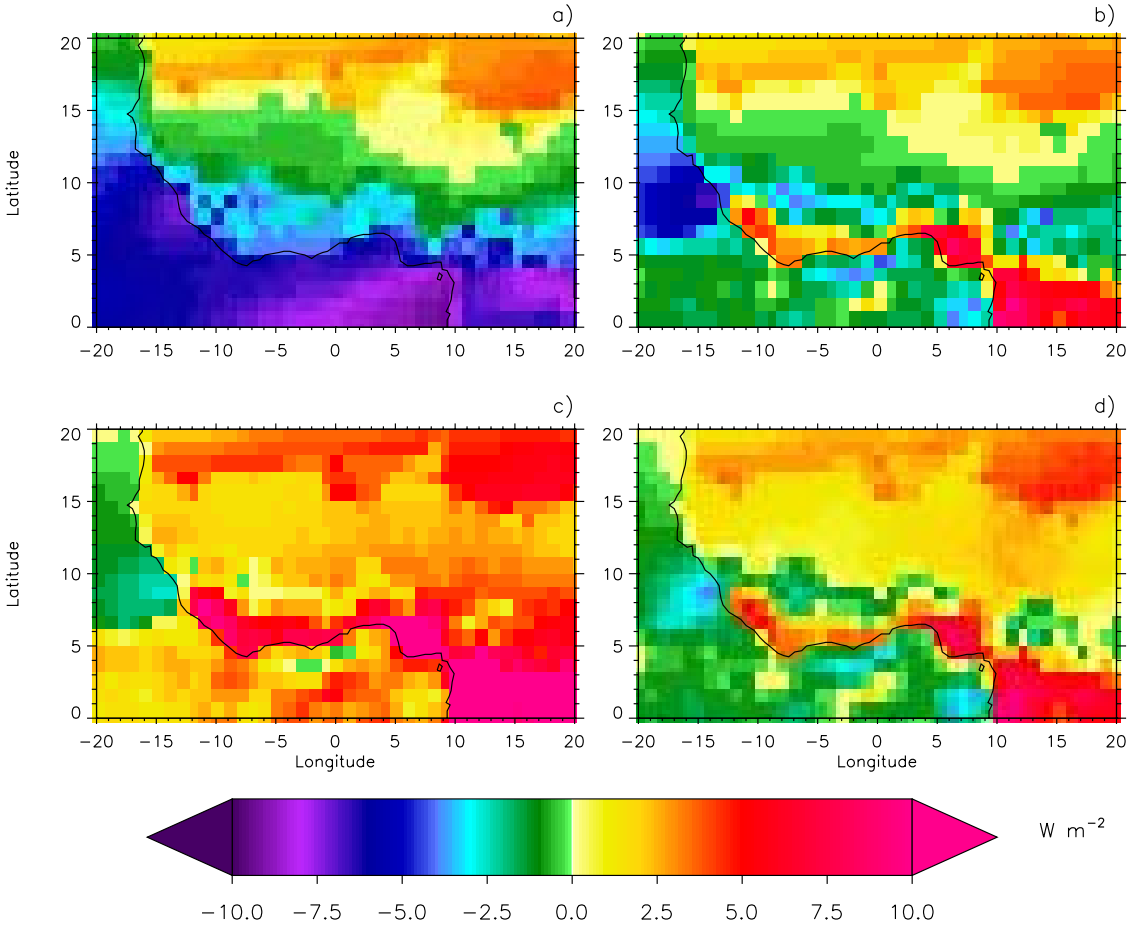

Figure 7. Radiative forcing at the top of the atmosphere due to BB aerosols during the DABEX campaign for (a) clear-sky conditions, (b) all sky, (c) all sky but the single scattering albedo of BB aerosols was reduced by 0.08, and (d) all sky but mineral dust was increased by a factor of 4 below 2 km. The mean over the region shown is −2.1, 0.06, 3.4, and 1.2 W m^{-2} for Figures 7a, 7b, 7c, and 7d, respectively.

radiative forcing was 3.4 W m^{-2} and areas of negative radiative forcing were almost completely eliminated (Figure 7c). Increasing the concentration of dust below 2 km increased the radiative forcing slightly (Figure 7d). This led to a positive regional mean forcing of 1.2 W m^{-2}. This also changes the radiative forcing from slightly negative to slightly positive over the region close to Niamey where the DABEX observations were made. Both sensitivity simulations increased the radiative forcing, with a particularly sensitivity to the change in the single scattering albedo. The uncertainty in the regional mean radiative forcing based on the sensitivity simulations is more than 3 W m^{-2}.

4. Summary

[19] To improve estimates of the direct aerosol effect and to reduce uncertainties associated with this it is vital that the global aerosol models are constrained by observations. We show here an example of how observations from a large aerosol campaign are brought into a global aerosol model.

[20] The modeled AOD compares reasonably well to measurements from AERONET stations near the main DABEX area (within 15–20% of monthly mean values). However, MODIS and MISR measurements indicate that the modeled AOD is too high in central Africa. This bias is likely to be related to excessive emissions over central Africa in the model. Another possibility is that the satellite retrievals miss some episodes of very high AOD, a problem that was observed during the SHADE campaign [*Haywood et al.*, 2003a; *Myhre et al.*, 2005]. We use aircraft observations from DABEX to specify the SSA of BB aerosols in the model. Compared to AERONET measurements, the model overestimates the column values of SSA, although the AERONET column values seem too low when compared with the aircraft observations. The aircraft data suggested that about 65% of the aerosol optical depth, during DABEX, was related to mineral dust [*Johnson et al.*, 2008b] and that the SSA of dust was around 0.98–0.99 [*Osborne et al.*, 2008]. Column-mean SSAs measured by the aircraft were typically around 0.90 at 550 nm, which is much higher than the AERONET observations from Banizoumbou (0.84 at 550 nm). It is important to resolve this difference between the SSA from the aircraft observations and AERONET since the SSA substantially affected the regional radiative forcing of the BB aerosol in this study. Comparison of AOD and SSA between the model and

AERONET indicate that the model reproduces the mixture of mineral dust and BB aerosols reasonably well.

[21] During DABEX the SSA increases with wavelength from 550 nm to 870 nm, which is the opposite tendency to that observed during SAFARI 2000. This may be explained by the strong decrease of BB AOD with wavelength, and the large mineral dust fraction during DABEX, which dominates aerosol optical properties more strongly at the longer wavelength. The wavelength dependence of SSA therefore gives an indication of whether mineral dust or BB aerosols dominate the aerosol column and may be a useful metric to compliment the more widely understood Ångstrøm exponent [*Tanré et al.*, 2003].

[22] The Oslo CTM2 does not successfully reproduce the observed vertical profile of aerosol in the lower part of the aerosol plume; it misses the large peak in dust and a sharp drop in BB aerosols below 2 km. The model profile of BB aerosols is more similar to observations made over southern Africa during SAFARI 2000 where a rather constant profile of BB aerosols from the surface to the top of the aerosol layer was observed [*Haywood et al.*, 2003b; *Myhre et al.*, 2003a]. The discrepancy between the model and observed aerosol profile, in the lowest 2 km during DABEX, could indicate a difference in the injection height of BB aerosol, compared to SAFARI 2000. Alternatively, the discrepancy could indicate that BB aerosols during DABEX mixed onto mineral dust at low altitudes and were therefore not observed by the aircraft since the aircraft analysis distinguished between dust and BB aerosols on the basis of the size distribution and Angstrom exponent. Another possibility is that the winds used to advect the biomass burning aerosol in the CTM may not be able to represent the detailed dynamical situation of the cold dry dust laden air associated with the Harmattan front which undercuts and lifts the warmer, moister, more unstable biomass burning aerosol-laden air to the south of the region [*Haywood et al.*, 2008].

[23] The radiative effect of biomass burning aerosols during the DABEX campaign in 2006 is simulated with Oslo CTM2. We simulate a very weak radiative effect of the BB aerosols on average over the campaign area, with local values little stronger than 10 W m^{-2}. The radiative effect depends on the aerosol content but also substantially on the underlying reflectance whether from the surface or from low cloud. Under clear-sky conditions the radiative effect of the BB aerosols has a strong cooling, except over the Saharan desert where surface reflectance is high. Two sensitivity simulations are performed on the basis of disagreement with observations, one with SSA values similar to the AERONET data instead of similar to the aircraft measurements and one simulation with increased mineral dust in the lowest 2 km in accordance with the aircraft measurements. In both simulations a positive regional mean TOA radiative forcing and positive radiative forcing near Niamey was simulated.

[24] **Acknowledgments.** We thank the principal investigators and their staff for establishing and maintaining the five AERONET sites used in this study. We appreciate the useful and constructive comments and suggestions from two reviewers. This study has received support from the Norwegian Research Council.

References

Abel, S. J., J. M. Haywood, E. J. Highwood, J. Li, and P. R. Buseck (2003), Evolution of biomass burning aerosol properties from an agricultural fire in southern Africa, *Geophys. Res. Lett.*, *30*(15), 1783, doi:10.1029/2003GL017342.

Berglen, T. F., T. K. Berntsen, I. S. A. Isaksen, and J. K. Sundet (2004), A global model of the coupled sulfur/oxidant chemistry in the troposphere: The sulfur cycle, *J. Geophys. Res.*, *109*, D19310, doi:10.1029/2003JD003948.

Bergstrom, R. W., P. Pilewskie, B. Schmid, and P. B. Russell (2003), Estimates of the spectral aerosol single scattering albedo and aerosol radiative effects during SAFARI 2000, *J. Geophys. Res.*, *108*(D13), 8474, doi:10.1029/2002JD002435.

Berntsen, T., et al. (2006), Abatement of greenhouse gases: Does location matter?, *Clim. Change*, *74*(4), 377–411, doi:10.1007/s10584-006-0433-4.

Derimian, Y., J.-F. Léon, O. Dubovik, I. Chiapello, D. Tanré, A. Sinyuk, F. Auriol, T. Podvin, G. Brogniez, and B. N. Holben (2008), Radiative properties of aerosol mixture observed during the dry season 2006 over M'Bour, Senegal (African Monsoon Multidisciplinary Analysis campaign), *J. Geophys. Res.*, *113*, D00C09, doi:10.1029/2008JD009904.

Eck, T. F., et al. (2003), Variability of biomass burning aerosol optical characteristics in southern Africa during the SAFARI 2000 dry season campaign and a comparison of single scattering albedo estimates from radiometric measurements, *J. Geophys. Res.*, *108*(D13), 8477, doi:10.1029/2002JD002321.

Forster, P., et al. (2007), Changes in atmospheric constituents and in radiative forcing, in *Climate Change 2007: The Physical Science Basis. Contribution of Working Group I to the Fourth Assessment Report of the Intergovernmental Panel on Climate Change*, edited by S. Solomon et al., pp. 129–234, Cambridge Univ. Press, Cambridge, U. K.

Giglio, L., et al. (2003), An enhanced contextual fire detection algorithm for MODIS, *Remote Sens. Environ.*, *87*(2–3), 273–282, doi:10.1016/S0034-4257(03)00184-6.

Grini, A., G. Myhre, C. S. Zender, and I. S. A. Isaksen (2005), Model simulations of dust sources and transport in the global atmosphere: Effects of soil erodibility and wind speed variability, *J. Geophys. Res.*, *110*, D02205, doi:10.1029/2004JD005037.

Hansen, J., M. Sato, and R. Ruedy (1997), Radiative forcing and climate response, *J. Geophys. Res.*, *102*(D6), 6831–6864, doi:10.1029/96JD03436.

Haywood, J. M., and K. P. Shine (1995), The effect of anthropogenic sulfate and soot aerosol on the clear-sky planetary radiation budget, *Geophys. Res. Lett.*, *22*(5), 603–606, doi:10.1029/95GL00075.

Haywood, J., P. Francis, S. Osborne, M. Glew, N. Loeb, E. Highwood, D. Tanré, G. Myhre, P. Formenti, and E. Hirst (2003a), Radiative properties and direct radiative effect of Saharan dust measured by the C-130 aircraft during SHADE: 1. Solar spectrum, *J. Geophys. Res.*, *108*(D18), 8577, doi:10.1029/2002JD002687.

Haywood, J. M., S. R. Osborne, P. N. Francis, A. Keil, P. Formenti, M. O. Andreae, and P. H. Kaye (2003b), The mean physical and optical properties of regional haze dominated by biomass burning aerosol measured from the C-130 aircraft during SAFARI 2000, *J. Geophys. Res.*, *108*(D13), 8473, doi:10.1029/2002JD002226.

Haywood, J. M., et al. (2008), Overview of the Dust And Biomass-burning Experiment and African Monsoon Multidisciplinary Analysis special observing period-0, *J. Geophys. Res.*, doi:10.1029/2008JD010077, in press.

Hoffmann, T., et al. (1997), Formation of organic aerosols from the oxidation of biogenic hydrocarbons, *J. Atmos. Chem.*, *26*(2), 189–222, doi:10.1023/A:1005734301837.

Holben, B. N., et al. (1998), AERONET—A federated instrument network and data archive for aerosol characterization, *Remote Sens. Environ.*, *66*(1), 1–16, doi:10.1016/S0034-4257(98)00031-5.

Hoyle, C. R., et al. (2007), Secondary organic aerosol in the global aerosol-chemical transport model Oslo CTM2, *Atmos. Chem. Phys.*, *7*, 5675–5694.

Ichoku, C., L. A. Remer, Y. J. Kaufman, R. Levy, D. A. Chu, D. Tanré, and B. N. Holben (2003), MODIS observation of aerosols and estimation of aerosol radiative forcing over southern Africa during SAFARI 2000, *J. Geophys. Res.*, *108*(D13), 8499, doi:10.1029/2002JD002366.

Johnson, B. T., et al. (2008a), Vertical distribution and radiative effects of mineral dust and biomass-burning aerosol over West Africa during DABEX, *J. Geophys. Res.*, *113*, D00C12, doi:10.1029/2008JD009848.

Johnson, B. T., S. R. Osborne, J. M. Haywood, and M. A. J. Harrison (2008b), Aircraft measurements of biomass burning aerosols over West Africa during DABEX, *J. Geophys. Res.*, *113*, D00C06, doi:10.1029/2007JD009451.

Kahn, R. A., B. J. Gaitley, J. V. Martonchik, D. J. Diner, K. A. Crean, and B. Holben (2005), Multiangle Imaging Spectroradiometer (MISR) global aerosol optical depth validation based on 2 years of coincident Aerosol Robotic Network (AERONET) observations, *J. Geophys. Res.*, *110*, D10S04, doi:10.1029/2004JD004706.

Keil, A., and J. M. Haywood (2003), Solar radiative forcing by biomass burning aerosol particles during SAFARI 2000: A case study based on

measured aerosol and cloud properties, *J. Geophys. Res.*, *108*(D13), 8467, doi:10.1029/2002JD002315.

Levy, R. C., L. A. Remer, S. Mattoo, E. F. Vermote, and Y. J. Kaufman (2007), Second-generation operational algorithm: Retrieval of aerosol properties over land from inversion of Moderate Resolution Imaging Spectroradiometer spectral reflectance, *J. Geophys. Res.*, *112*, D13211, doi:10.1029/2006JD007811.

Mallet, M., et al. (2008), Aerosol direct radiative forcing over Djougou (northern Benin) during the African Monsoon Multidisciplinary Analysis dry season experiment (Special Observation Period-0), *J. Geophys. Res.*, *113*, D00C01, doi:10.1029/2007JD009419.

Matichuk, R. I., P. R. Colarco, J. A. Smith, and O. B. Toon (2007), Modeling the transport and optical properties of smoke aerosols from African savanna fires during the Southern African Regional Science Initiative campaign (SAFARI 2000), *J. Geophys. Res.*, *112*, D08203, doi:10.1029/2006JD007528.

Milton, S. F., G. Greed, M. E. Brooks, J. Haywood, B. Johnson, R. P. Allan, A. Slingo, and W. M. F. Grey (2008), Modeled and observed atmospheric radiation balance during the West African dry season: Role of mineral dust, biomass burning aerosol, and surface albedo, *J. Geophys. Res.*, *113*, D00C02, doi:10.1029/2007JD009741.

Myhre, G., T. K. Berntsen, J. M. Haywood, J. K. Sundet, B. N. Holben, M. Johnsrud, and F. Stordal (2003a), Modeling the solar radiative impact of aerosols from biomass burning during the Southern African Regional Science Initiative (SAFARI-2000) experiment, *J. Geophys. Res.*, *108*(D13), 8501, doi:10.1029/2002JD002313.

Myhre, G., A. Grini, J. M. Haywood, F. Stordal, B. Chatenet, D. Tanré, J. K. Sundet, and I. S. A. Isaksen (2003b), Modeling the radiative impact of mineral dust during the Saharan Dust Experiment (SHADE) campaign, *J. Geophys. Res.*, *108*(D18), 8579, doi:10.1029/2002JD002566.

Myhre, G., et al. (2005), Intercomparison of satellite retrieved aerosol optical depth over ocean during the period September 1997 to December 2000, *Atmos. Chem. Phys.*, *5*, 1697–1719.

Myhre, G., et al. (2007), Comparison of the radiative properties and direct radiative effect of aerosols from a global aerosol model and remote sensing data over ocean, *Tellus, Ser. B*, *59*(1), 115–129, doi:10.1111/j.1600-0889.2006.00226.x.

Osborne, S. R., B. T. Johnson, J. M. Haywood, A. J. Baran, M. A. J. Harrison, and C. L. McConnell (2008), Physical and optical properties of mineral dust aerosol during the Dust and Biomass-burning Experiment, *J. Geophys. Res.*, *113*, D00C03, doi:10.1029/2007JD009551.

Remer, L. A., et al. (2005), The MODIS aerosol algorithm, products, and validation, *J. Atmos. Sci.*, *62*(4), 947–973, doi:10.1175/JAS3385.1.

Schulz, M., et al. (2006), Radiative forcing by aerosols as derived from the AeroCom present-day and pre-industrial simulations, *Atmos. Chem. Phys.*, *6*, 5225–5246.

Schwarz, J. P., et al. (2006), Single-particle measurements of midlatitude black carbon and light-scattering aerosols from the boundary layer to the lower stratosphere, *J. Geophys. Res.*, *111*, D16207, doi:10.1029/2006JD007076.

Stamnes, K., et al. (1988), Numerically stable algorithm for discrete-ordinate-method radiative-transfer in multiple-scattering and emitting layered media, *Appl. Opt.*, *27*(12), 2502–2509.

Swap, R. J., H. J. Annegarn, J. T. Suttles, M. D. King, S. Platnick, J. L. Privette, and R. J. Scholes (2003), Africa burning: A thematic analysis of the Southern African Regional Science Initiative (SAFARI 2000), *J. Geophys. Res.*, *108*(D13), 8465, doi:10.1029/2003JD003747.

Tanré, D., J. Haywood, J. Pelon, J. F. Léon, B. Chatenet, P. Formenti, P. Francis, P. Goloub, E. J. Highwood, and G. Myhre (2003), Measurement and modeling of the Saharan dust radiative impact: Overview of the Saharan Dust Experiment (SHADE), *J. Geophys. Res.*, *108*(D18), 8574, doi:10.1029/2002JD003273.

Textor, C., et al. (2006), Analysis and quantification of the diversities of aerosol life cycles within AeroCom, *Atmos. Chem. Phys.*, *6*, 1777–1813.

van der Werf, G. R., et al. (2006), Interannual variability in global biomass burning emissions from 199 7 to 200 4, *Atmos. Chem. Phys.*, *6*, 3423–3441.

T. F. Berglen and C. R. Hoyle, Department of Geosciences, University of Oslo, NO-0316 Oslo, Norway.

J. M. Haywood and B. T. Johnson, Met Office, Exeter EX1 3PB, UK.

G. Myhre, Center for International Climate and Environmental Research-Oslo, NO-0318 Oslo, Norway. (gunnar.myhre@cicero.uio.no)